Surface Vibrations of Large Water Clusters by He Atom Scattering

Jesko Brudermann, Petra Lohbrandt, and Udo Buck
Max-Planck-Institut für Strömungsforschung, Bunsenstraße 10, D-37073 Göttingen, Germany

Victoria Buch
The Fritz Haber Institute for Molecular Dynamics, The Hebrew University, Jerusalem 91904, Israel

(Received 31 October 1997)

The low energy intermolecular vibrational modes of water clusters for the average size $\overline{n} = 110$ have been measured by high resolution inelastic helium atom scattering. The water clusters are generated in adiabatic expansions through conical nozzles. By accompanying quantum and classical calculations the excited mode at 5.0 meV has been identified as O· ·O· ·O bending motion between adjacent hydrogen bonds, involving 3-coordinated water molecules on the amorphous cluster surface. Experiments for different sizes show that the frequency and thus the force constant of this mode increase for larger cluster sizes. [S0031-9007(98)05739-1]

PACS numbers: 36.40.Sx, 34.50.Dy, 68.35.Ja

Weakly bonded clusters have been a focus of intense interest during the past few years. One of the major objectives is to understand how the particles evolve as a function of size towards condensed phase behavior. The evolution of particle properties is influenced strongly by the large surface-to-bulk ratio, and therefore experimental tools sensitive specifically to the cluster surface properties are of interest. A unique tool of this kind has been developed in our laboratory, which probes surface vibrations by inelastic energy exchange with He atoms scattered from the particles [1]. In fact, we were able to demonstrate that in helium atom - argon cluster collisions surface modes were predominantly excited [2]. One can distinguish between single phonon and multiphonon excitation [3] using the measured angular dependence, in conjunction with calculations. Here the method is applied to the investigation of vibrational surface properties of water particles. Water clusters are of particular interest because of the importance of water in terrestrial phenomena, and because of the role of icy particles in atmospheric and extraterrestrial physics and chemistry. Electron diffraction studies of $(H_2O)_n$ up to sizes of several hundred molecules demonstrated a noncrystalline structure [4], while spectroscopic studies of ice nanocrystal surfaces and surface-adsorbate systems showed persistence of amorphous surface structure to larger sizes, for which the particle interior is crystalline [5]. Thus, past studies indicate the properties of small ice particles that are quite distinct from those of bulk ice, and surface properties that are distinct from the interior. The present study focuses on these aspects of cluster behavior, for low energy, hydrogen bond vibration frequencies.

For bulk hexagonal ice these modes have been measured by neutron scattering. In the range from 2 to 40 meV the peaks are attributed to the hindered intermolecular motion and interpreted as acoustical (7.1 meV) and optical (28.4 and 37.9 meV) modes [6], the splitting between the latter ones still being a subject of controversy [6,7]. The modes near 7.1 meV have also been interpreted as O· ·O· ·O bending between adjacent hydrogen bonds [8], while the higher frequency modes have been assigned to hydrogen bond stretching [6,8]. For clusters, extensive calculations are available for some selected small species [9,10]. Here we present the first measurements of water clusters for the average size of $\overline{n} = 110$. We concentrate on the excitation of the low energy vibrational modes which are detected by time-of-flight (TOF) analysis of the scattered helium atom. By comparison of the data with calculations of the density of states and their excitation probability in helium collisions, we were able to identify unambiguously the type of cluster excitations.

The experiments have been carried out in a crossed molecular beam machine which is described in detail elsewhere [11]. The helium atom and the $(H_2O)_n$ cluster beam are generated in separated, differentially pumped source chambers and intersect each other under 90° in the scattering chamber. The angular dependence of the scattered intensity is measured by rotating the source assembly around the scattering center, while the detector unit, consisting of an electron impact ionizer combined with a quadrupole mass filter and a secondary electron multiplier, is kept fixed. The velocity of the scattered helium atoms is measured by time-of-flight analysis using a pseudorandom chopper, located between the scattering center and the detector, with a flight path of 450 mm.

The helium atom beam is produced by expansion of the gas under high stagnation pressure of 15 bars through a small orifice with a diameter of 30 μm at a source temperature of $T_0 = 77$ K. Under these conditions the relative width of the velocity distribution is $\Delta v/v = 0.017$ which leads to the energy resolution between 2 and 4 meV at a collision energy of about 62.5 meV. The $(H_2O)_n$-cluster beam is generated by expansion of water vapor at 10 bars through a conical nozzle with a diameter of 70 μm, an opening angle of 35° and 2 mm length at a temperature of $T = 621$ K. The beam contains a distribution of cluster sizes, which we have analyzed using a reflectron time-of-flight mass spectrometer in which the $(H_2O)_n$ clusters are ionized by single photon ionization after they have been doped by one sodium atom [12]. The measured sizes follow a log-normal distribution with an average cluster size of $\overline{n} = 110$ and about the same half-width.

The information on the vibrational excitation is directly obtained from the time-of-flight spectra measured at different laboratory (lab) scattering angles Θ. A typical example of such a measurement at the collision energy of $E = 62.5$ meV is shown in Fig. 1. The three selected lab angles 11°, 15°, and 20° are close to the minima of the total differential cross section curve which contains contributions of the scattered clusters and remaining monomers. This observable is dominated by the diffraction oscillations of scattered monomers, and near their minima we expect the largest contributions from the clusters [2]. In contrast to the results obtained for argon [2] and ammonia [13] clusters, the spectra exhibit three well-resolved peaks. In order to assign these peaks, we first calculate the corresponding energy transfer. From the measured primary and target beam velocities and the transformation from the center-of-mass to the laboratory system, the velocities of the scattered helium atoms are calculated for the different energy transfers ΔE. The first peak is close to where we expect the elastic scattering of monomers (m) and clusters (c), as indicated by the arrows. The possible inelastic contributions then appear with increasing energy loss. Here we have marked the peaks by the corresponding loss in meV. We essentially observe two additional features, a middle peak with an average energy loss of about 5 meV, nearly independent of the deflection angle, and a peak at larger energy transfers which varies from 14 to 22 meV with increasing deflection angle. Since the latter peak is also present at deflection angles which are dominated by monomer scattering, we attribute it to inelastic monomer scattering and concentrate on the middle peak as the cluster contribution.

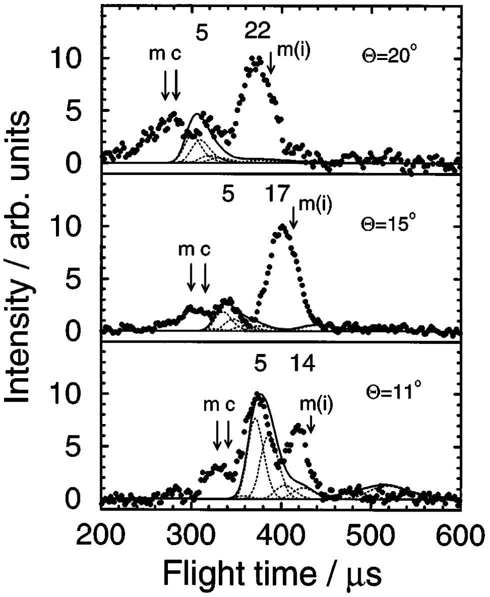

FIG. 1. Measured time-of-flight spectra for water clusters of the averaged size of $\overline{n} = 110$ taken at three different laboratory angles. The position of elastically scattered monomers (m) and clusters (c) and inelastically scattered monomers $[m(i)]$ are indicated by arrows. The lines (solid line: sum; dotted line: single contributions) are calculated inelastic cross sections of He + $(H_2O)_{90}$ collisions as are shown in Fig. 2(b). The numbers indicate the energy transfer in meV of the peaks below.

In order to substantiate this picture we have carried out computer simulations of this system. Up to now, such calculations have only been performed for the scattering of He from Ar_n clusters [3,14]. The results clearly demonstrated that quasiclassical trajectories are not sufficient to describe correctly the energy transfer of single phonon excitations. On the other hand, the quantum mechanical treatment of such a high dimensional coupled system requires approximations. Here we have chosen an approach which is closely related to the semiclassical forced oscillator model [15].

The complete procedure for the scattering calculation involves three steps: (i) The generation of a water cluster in the measured size range, here $n = 90$, (ii) the calculation of the vibrational frequency distribution, and (iii) the calculation of the differential scattering cross section for the excitation of single quanta in collisions with helium.

We will discuss these steps separately. The calculations employed an approximately spherical water cluster model of 90 molecules that was prepared by "cutting" a sphere from the cubic ice structure, annealing it at 150 K, and cooling it down to 80 K by molecular dynamics (MD). The resulting cluster is amorphous. The water potential employed in all the calculations was TIPS2 [16]. The classical MD does not provide a good description of inelastic phonon excitation, which is essentially a quantum-mechanical process. The reason is that in classical mechanics any amount of energy can be transferred to any vibrational mode, while in quantum mechanics energy transfer occurs in discrete quanta. To account for that fact we proceeded as follows. First, the normal mode analysis was carried out at the cluster minimum. Then, classical trajectories were calculated for a He atom colliding at random with the cluster in its minimum configuration. For the atom-cluster interaction a pair additive Lennard-Jones He-H_2O potential was used [17]. The excitation probability $P_{j,0\to 1}$ of each normal mode j from the ground state $v = 0$ to the first excited state $v = 1$ was calculated using time dependent perturbation theory. The perturbation was assumed linear in the normal mode displacement and calculated from the classical trajectory

[18], giving

$$P_{j,0\to 1} = \frac{1}{2\hbar\omega}\left|\sum_i F_i(\omega_j)a_{ij}\right|^2 . \qquad (1)$$

$F_i(\omega)$ is the Fourier transform of the perturbation and a_{ij} are the transformation matrix elements from the Cartesian O-atom displacements to normal coordinates. We get the differential cross sections by summing over contributions from normal mode excitations by trajectories which lead into different deflection angles.

A typical result of such a calculation is shown in the upper parts of Fig. 2. Figure 2(a) exhibits the frequency distribution based on the normal mode analysis. We see mainly two peaks centered at about 5 to 10 meV and 25 to 35 meV. Figure 2(b) displays a histogram of phonon energies that were excited in collisions with helium at the energy of 65 meV and a deflection angle of 17.5°, in the center-of-mass (c.m.) system. The results are very similar up to c.m. deflection angles of about 50°. In all cases, only the lowest energy part of the frequency distribution is excited.

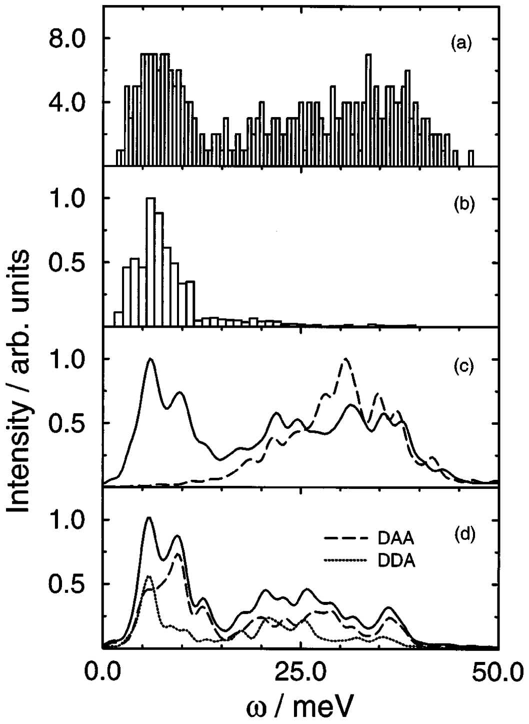

FIG. 2. (a) Distribution of cluster frequencies, obtained from normal mode analysis. (b) A histogram of phonon energies excited in collisions with helium at the energy of 65 meV and a deflection angle of 17.5°, in the center-of-mass system. (c) Fourier transform of the autocorrelation function for the hydrogen bond stretch O· ·O (dashed line), and for the bending between adjacent hydrogen bonds O· ·O· ·O (solid line), obtained from a classical trajectory simulation of the cluster, and averaged over all cluster molecules. (d) Solid line: Fourier transform of the autocorrelation function for O· ·O· ·O bending; the middle O atom belongs to a molecule that was approached most closely by He in one of the collision trajectories. Dashed line: contribution to the spectrum from DAA molecules. Dotted line: contribution from DDA.

Now we compare these results directly with the measurements. For that purpose the calculated double differential cross sections are transformed into time-of-flight spectra. In this procedure the averaging processes of the apparatus are properly taken into account. The experimental resolution function is calculated in a Monte Carlo procedure using the measured width of the velocity distributions, the angular divergences of the two intersecting beams, the finite dimension of the scattering volume, the detector, and the resolution of the TOF analyzer [19]. Based on this function, which also contains the transformation from the center-of-mass to the laboratory system, we calculate directly the TOF spectra. The results are shown in Fig. 1 as the solid lines. The dotted lines indicate the single contributions of the excited modes for every 2 meV interval. The middle peak of the spectrum is well reproduced for all three lab angles. Thus we conclude that this peak is caused by the excitation of the low energy vibrations of the clusters.

Having explained the meaning of the first and second peaks, we are left with the explanation of the third peak which exhibits, in contrast to the second one, a variable energy transfer as a function of the angle. The explanation that this peak is caused by multiphonon excitation of the clusters is quite improbable. Test calculations show that the angular range investigated here is too small for an appreciable amount of overtone excitations. In addition, it should lead to a constant excitation as a function of angle, as does the excitation of the fundamental. However, quasiclassical trajectory simulations of He + H_2O monomer collisions, employing a realistic *ab initio* potential surface [20], give indeed inelastic contributions which peak as a function of the deflection angle at the values marked $m(i)$ in Fig. 1 by arrows. The general trend of this excitation is quite well reproduced. Past studies suggest that the classical treatment of atom-molecule collisions is reasonable for rotationally inelastic transitions at energies well above the excitation threshold [21]. The discrepancies left in the absolute position might be a consequence of inaccuracies in the potential or in the classical treatment.

We now focus on the assignment of cluster motions that are excited by the collisions with the He atoms. From comparison of Figs. 2(a) and 2(b) it is seen that collisions excite preferentially the low frequency part of the first peak in the density of frequencies. To assign this peak, calculations were carried out in classical trajectories for the cluster, followed by an evaluation of frequency spectra for different types of molecular motions. Specifically, the Fourier transform of the autocorrelation function was calculated for the hydrogen bond stretch O· ·O and for the bending motion between adjacent hydrogen bonds O· ·O· ·O. Figure 2(c) shows the spectra, averaged over all of the hydrogen bonds in the cluster. In accordance with the suggestion of [8], the first peak in the frequency spectrum is contributed predominantly by the O· ·O· ·O bending. More relevant to the excitation by collisions is the bending spectrum for those water molecules which were hit by He atoms during the trajectories. Figure 2(d) shows the spectrum of the O· ·O· ·O bending angles, such that the middle O atom belongs to a molecule which was approached most closely by He in one of the collision trajectories. While the overall shape of the surface bending spectrum is similar to the "all cluster" one shown in Fig. 2(c), its two major contributions originate from 3-coordinated water molecules that are characteristic of the cluster *surface*. One should note at this point that more than half of the cluster molecules are 4-coordinated, while most of the molecules hit by the impinging He atoms are 3-coordinated; this result is not surprising, considering that 3-coordinated molecules tend to protrude from the surface. The 3-coordinated molecules come in two varieties: (a) double proton donor, single acceptor (DDA); and (b) single donor, double acceptor (DAA). It is seen in Fig. 2(d) that the DDA spectrum peaks at 5 meV. The DAA spectrum peaks at 10 meV, but has a substantial wing at 5 meV as well. Comparison of the excitation spectrum in Fig. 2(c) with the frequency spectra in Figs. 2(a) and 2(d) shows that collisions excite preferentially the lower frequency part of the bending spectrum, near 5 meV, in accordance with the experiment. The preference for the lower frequency bending modes is caused by the factor $1/\omega$ in Eq. (1).

We conclude that the peak at 5.0 meV, which is measured in the experiment, is essentially caused by collisional excitation of the bending motion of 3-coordinated surface water molecules. Interestingly, the measured peak frequency remains about the same down to $\overline{n} = 20$. At even smaller sizes at about $\overline{n} = 10$, the spectrum broadens and contains energies between 4 and 6 meV. At larger sizes $\overline{n} = 200$, the peak excitation frequency increases slightly to 5.5 meV. This value is still somewhat lower than the peak frequency of 5.9 meV, measured recently by He scattering from the crystalline ice surface [22]. The lower cluster value is consistent with the amorphous surface structure expected for water clusters in this size range [4,5]. Thus we have for this low energy bending mode a hierarchy of frequencies and correlated force constants which start with 7.1 meV of 4-coordinated bulk ice, go over to 5.9 meV for 3-coordinated surface molecules of crystalline ice, and end with 5.0 meV for 3-coordinated surface molecules of amorphous clusters between $\overline{n} = 20$ and 100. This result is in contrast to the findings for Ar_n clusters for which the energy of the lowest frequency mode, identified as collective breathing motion, decreases with increasing size [1]. Obviously, the water molecules behave differently, and the result suggests that in smaller clusters the strain in the hydrogen bond network reduces the effective bending force constant.

We acknowledge the financial support from the Deutsche Forschungsgemeinschaft, and the Israel Academy of Science.

[1] U. Buck and R. Krohne, Phys. Rev. Lett. **73**, 947 (1994).

[2] U. Buck, R. Krohne, and P. Lohbrandt, J. Chem. Phys. **106**, 3205 (1997).

[3] T. Schröder, R. Schinke, U. Buck, and R. Krohne, J. Chem. Phys. **106**, 9067 (1997).

[4] G. Torchet, P. Schwartz, J. Farges, M. F. de Feraudy, and B. Raoult, J. Chem. Phys. **79**, 6196 (1983).

[5] V. Buch, L. Delzeit, C. Blackledge, and J. P. Devlin, J. Phys. Chem. **100**, 10 076 (1996); B. Rowland, S. Kadagathur, J. P. Devlin, V. Buch, T. Feldmann, and M. Wojcik, J. Chem. Phys. **102**, 8328 (1995).

[6] J. C. Li, J. Chem. Phys. **105**, 6733 (1996).

[7] D. D. Klug, J. S. Tse, and E. Whalley, J. Chem. Phys. **95**, 7011 (1991).

[8] M. G. Sceats and S. A. Rice, J. Chem. Phys. **72**, 3236 (1980).

[9] R. Knochenmuss and S. Leutwyler, J. Chem. Phys. **96**, 5232 (1992).

[10] J. O. Jung and R. B. Gerber, J. Chem. Phys. **105**, 10 332 (1996).

[11] U. Buck, F. Huisken, J. Schleusener, and J. Schaefer, J. Chem. Phys. **72**, 1512 (1980).

[12] C. Bobbert, U. Buck, and S. Schütte (unpublished).

[13] U. Buck, R. Krohne, and S. Schütte, J. Chem. Phys. **106**, 109 (1997).

[14] A. Y. Rom and R. B. Gerber, J. Chem. Phys. **106**, 10 168 (1997).

[15] M. Persson and J. Harris, Surf. Sci. **187**, 67 (1987).

[16] W. L. Jorgensen, J. Chem. Phys. **77**, 4156 (1982).

[17] R. W. Bickes, Jr., G. Duquette, C. J. N. van der Meijdenberg, A. M. Rulis, G. Scoles, and K. M. Smith, J. Phys. B **8**, 3034 (1975).

[18] C. Cohen-Tannoudji, B. Diu, and F. Laloë, *Quantum Mechanics* (John Wiley, Paris, 1977), Vol. 2, Chap. 13.

[19] U. Buck, in *Atomic and Molecular Beam Methods*, edited by G. Scoles (Oxford, New York, 1988), Chap. 21, p. 525.

[20] S. Greene, D. J. Forbes, and A. D. McLean, J. Chem. Phys. **94**, 1346 (1991).

[21] S. Lepp, V. Buch, A. Dalgarno, Astrophys. J. Suppl. **98**, 345 (1995).

[22] J. Braun, A. Glebov, A. P. Graham, A. Menzel, and J. P. Toennies, Phys. Rev. Lett. (to be published).